Engineering Science & Technology
https://ojs.wiserpub.com/index.php/EST/

UNIVERSAL WISER PUBLISHER

Research Article

Harnessing Soil Organic Carbon to Build a More Productive and Climate-Resilient Future

Sanjay Saxsena[1], Saurabh Kumar Gupta[1], Shruti Kanga[2], Suraj Kumar Singh[1], Pankaj Kumar[3*], Gowhar Meraj[4], Sudhanshu[1]

[1]Centre for Climate Change and Water Research, Suresh Gyan Vihar University, Jaipur, Rajasthan, 302017, India
[2]Department of Geography, School of Environment and Earth Sciences, Central University, Punjab, 151401, India
[3]Institute for Global Environmental Strategies, Hayama, 240-0115, Japan
[4]Department of Biology, Chemistry and Environmental Sciences, American University of Sharjah, Sharjah Emirate, 26666, United Arab Emirates
E-mail: mjhadad@ut.ac.ir

Received: 15 September 2025; **Revised:** 10 November 2025; **Accepted:** 27 November 2025

Abstract: Soil Organic Carbon (SOC) is a critical determinant of soil fertility, ecosystem stability, and climate regulation. This study analyzes the spatial and temporal dynamics of SOC in the Tonk District of Rajasthan, India, using the Trend.Earth platform integrated with satellite-derived Land-Use and Land-Cover (LULC) data for the period 2001-2020. Statistical trend analyses (Mann-Kendall, Sen's Slope, and Pearson correlation) indicate that 98.31% ± 0.17% of the area has remained stable in SOC content, demonstrating high soil resilience, while 1.63% ± 0.17% shows measurable degradation, largely influenced by wind erosion and intensive agricultural activity. Land-use transition analysis further reveals 54.79 km^2 of urban expansion and 114.52 km^2 of reduced irrigated cropland, reflecting growing anthropogenic pressure on soil resources. These findings emphasize the need for targeted soil conservation, agro-forestry adoption, and integrated land-management policies to sustain soil carbon stocks. The study demonstrates the applicability of Trend. Earth-based geospatial monitoring for evidence-driven SOC assessment and regional climate resilience planning in semi-arid environments

***Keywords*:** Soil Organic Carbon (SOC), land use change, wind erosion, Trend.Earth, climate resilience

1. Introduction

Soil Organic Carbon (SOC) is a fundamental cornerstone of global soil health and a critical regulator of the planet's climate [1]. As the largest terrestrial carbon pool, SOC is indispensable for maintaining soil fertility, enhancing water retention, and supporting overall ecosystem function, all of which are vital to global food security. Despite its significance, this vital resource is increasingly vulnerable to degradation, primarily driven by unsustainable land management practices and rapid Land Use and Land Cover (LULC) changes globally [2].

LULC change, including deforestation, agricultural expansion, and urbanization, is the most significant anthropogenic driver, altering SOC dynamics. The conversion of natural ecosystems to intensive cropland, for instance, typically results in substantial SOC losses-often 20-50% within decades-due to reduced organic matter input, accelerated

DOI: https://doi.org/10.37256/est.7120268634

decomposition rates, and soil structural disruption [3], [4]. Agricultural intensification within existing systems further exacerbates depletion through excessive tillage, residue removal, and monoculture dominance [5]. Conversely, sustainable practices such as conservation agriculture, agroforestry, and cover cropping offer significant potential for SOC sequestration by minimizing disturbance, maintaining perennial cover, and increasing organic inputs [6], [7].

Beyond LULC, environmental processes such as wind erosion-particularly prevalent in arid and semi-arid regions-act as a major cause of SOC loss by selectively removing carbon-rich topsoil particles [8], [9]. Furthermore, extractive industries like mining physically disturb the soil profile, strip vegetation, and fragment landscapes, leading to severe localized SOC depletion and long-term ecosystem dysfunction [10]. A nuanced understanding of these dynamics requires analyzing not only major transitions between land-use types (e.g., forest to cropland) but also changes within a single class, such as the intensification of agriculture [11].

While global research confirms the importance of SOC and its vulnerability, comprehensive national-scale assessments are often lacking, particularly in regions facing compounded threats. In India, studies have assessed SOC status across various agro-ecological zones [12], yet significant research gaps remain regarding the combined effects of multiple drivers at high spatial resolution. Specifically, the interplay between wind erosion dynamics, LULC patterns, and SOC vulnerability in India's semi-arid regions, like Rajasthan, is not yet well-quantified [13]. Similarly, the precise impacts of mining, urban expansion, and the efficacy of local mitigation strategies require more rigorous, data-driven validation. Modern platforms like Trend.Earth leverage Earth observation data, cloud computing, and advanced analytical tools to provide a robust framework for assessing and monitoring land change, including SOC trends [14]-[16]. Yet, the application of this powerful tool for studying the complex SOC-LULC and environmental driver interactions in Indian drylands remains limited.

This study aims to bridge this gap by leveraging the Trend.Earth platform to analyze SOC trends over the period 2000-2020 in Tonk district, Rajasthan-a semi-arid region characterized by aeolian soils, rainfed agriculture, and expanding mining activity. We aim to quantify concurrent LULC transitions and transformations, correlate these with key environmental drivers (wind erosion, mining extent), and identify degradation hotspots. We hypothesize that SOC degradation hotspots in Tonk coincide with areas of high wind erosion vulnerability and specific land-use transitions (e.g., natural vegetation loss to intensive agriculture or mined land).

The specific objectives of this study are fourfold. First, to map the spatiotemporal changes in SOC stocks across the study area using the Trend.Earth soil carbon module, enabling detection of long-term degradation and recovery patterns. Second, to quantify LULC transitions, along with within-class intensification trends, such as the expansion of croplands and the proliferation of mining areas. Third, to assess the correlations between SOC loss, wind exposure, and land-use trajectories, thereby identifying the key drivers influencing soil carbon dynamics. Finally, the study aims to propose targeted, evidence-based interventions for SOC restoration and promote climate-resilient land management practices tailored to the local ecological and socio-economic context.

The findings will inform the development of targeted, evidence-based policies and sustainable land management practices necessary for mitigating SOC loss, enhancing soil health, and bolstering ecosystem resilience in India's challenging dryland environment. This integrated approach will support Rajasthan's climate resilience strategies and serve as a scalable model for other semi-arid regions globally.

2. Study area, methodology, and data used

2.1 *Study area*

Tonk district is situated in the eastern part of Rajasthan, India, between approximately 25.4° N to 26.5° N latitude and 75.1° E to 76.2° E longitude. The region experiences a semi-arid climate (Agro-Climatic Zone III-A) with a mean annual rainfall of approximately 500 mm [17], concentrated during the Southwest Monsoon (June-September). The climate is characterized by high potential evapotranspiration and frequent pre-monsoon dust storms, which significantly exacerbate the risk of soil erosion. The dominant soil orders in the district are Inceptisols and Aridisols, which are typically sandy loam to alluvial in nature. These soils are inherently low in Organic Carbon (OC) (often ranging from 0.2% to 0.5% in surface soils) and are highly susceptible to wind-driven topsoil loss [18]. Agriculture remains the economic backbone, with major crops including wheat, mustard, and gram cultivated under predominantly rainfed

systems. Vegetation cover is naturally sparse, consisting of dry deciduous scrub and thorny species, reflected in generally low to moderate NDVI values. Expanding stone and minor mineral mining, along with gradual urbanization, further contributes to landscape fragmentation and soil disturbance. Tonk is therefore a highly representative case study for India's semi-arid dryland, where the critical issues of low Soil Organic Carbon (SOC) stocks, intense wind erosion, and land-use intensification converge to challenge long-term land productivity. Figure 1 shows the study area map of Tonk, Rajasthan.

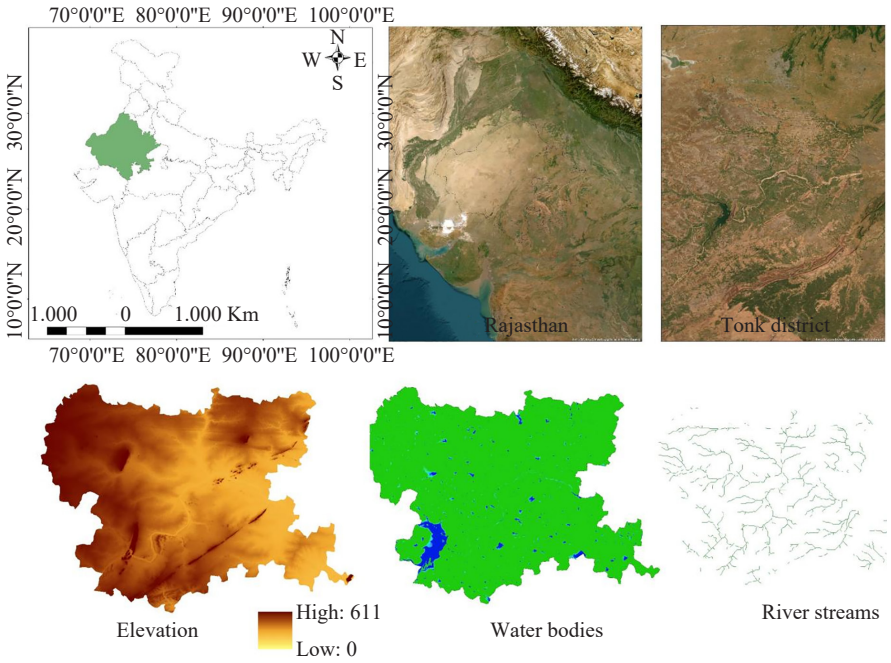

Figure 1. Study area map: Tonk, Rajasthan

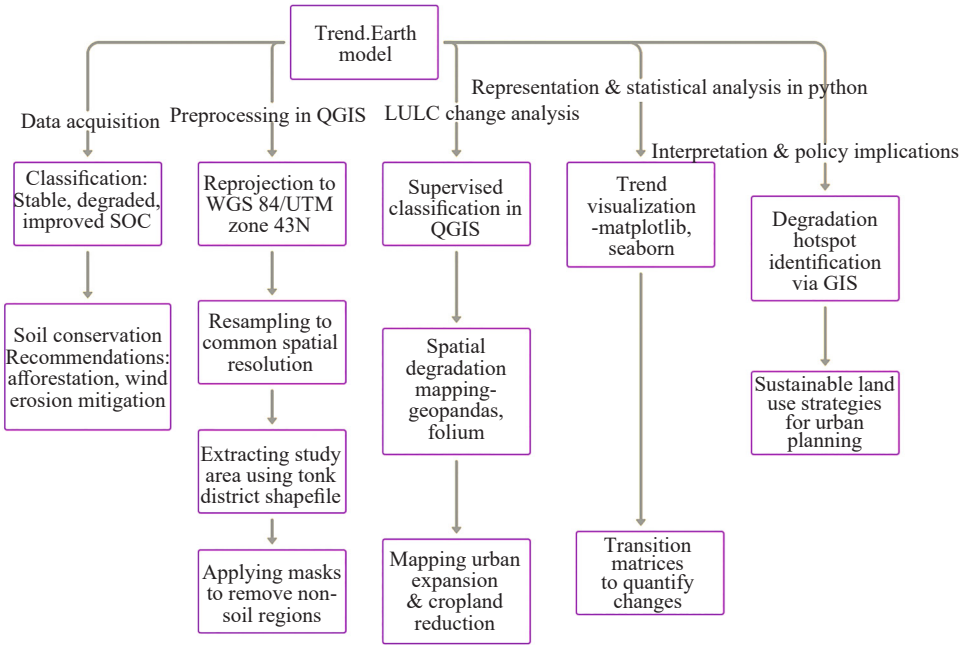

Figure 2. Methodological workflow: (a) data acquisition and preprocessing, (b) Random forest LULC classification, (c) SOC trend and hotspot detection, (d) transition matrix analysis, (e) statistical integration and policy outputs

This study integrates remote sensing, machine learning, field validation, and statistical analysis to assess Soil Organic Carbon (SOC) trends and their linkages to Land Use/Land Cover (LULC) changes and environmental drivers in Tonk district, Rajasthan. All spatial data were processed at 30 m resolution in the WGS 84/UTM Zone 43N (EPSG: 32643) projection using QGIS 3.34 and Python 3.10. The analytical workflow is summarized in Figure 2.

2.2 *Data acquisition and preprocessing*

Key datasets were acquired from global and regional repositories (Table 1). SOC stock data (2001-2020) were obtained from Trend.Earth (SDG 15.3.1 indicator), originally at 300 m resolution and resampled to 30 m using bilinear interpolation. LULC maps for 2001 and 2020 were harmonized from MODIS MCD12Q1 (500 m) and ESA WorldCover (10 m) through legend cross-walking and majority filtering. Wind speed and direction were derived from ERA5-Land reanalysis (0.1°), interpolated to 30 m. The Tonk district boundary (Survey of India, 2020) was used to clip all layers. Urban areas and permanent water bodies were masked from SOC trend analysis but retained in LULC transition matrices to quantify urbanization impacts.

Table 1. Data sources and specifications

Data Type	Source	Temporal coverage	Native resolution	Processed resolution	Key variables
SOC	Trend.Earth	2001-2020	300 m	30 m	SOC stock ($t \cdot C \cdot ha^{-1}$), trend
LULC	ESA worldcover, MODIS MCD12Q1	2001, 2020	10 m, 500 m	30 m	7 classes (cropland, grassland, tree cover, shrubland, bare, urban, water)
Wind	ERA5-land (ECMWF)	2001-2020	0.1°	30 m	*u*/*v* wind components
Topography	SRTM DEM	Static	30 m	30 m	Elevation, slope
Soil	NBSS & LUP	Static	1 : 250,000	30 m	Texture (sandy loam dominant)

2.3 *LULC classification and validation*

A Random Forest (RF) classifier was implemented in Python (scikit-learn v1.3) to refine and validate LULC maps. Training was based on 1,200 reference points collected via stratified random sampling from high-resolution Google Earth imagery (2020-2021). Predictor variables included spectral bands from ESA WorldCover and seasonal NDVI metrics from MOD13Q1. Model hyperparameters were set as: n_estimators = 500, max_depth = 20, min_samples_split = 5, and random_state = 42. An independent validation using 400 points yielded an Overall Accuracy (OA) of 87.6% and a Kappa coefficient (κ) of 0.81. Class-wise producer and user accuracies are provided in Table S1 (Appendix Material).

2.4 *SOC trend and hotspot analysis*

Annual SOC stock change (ΔSOC) was calculated as (1):

$$\Delta SOC_{2001–2020} = SOC_{2020} - SOC_{2001} \quad (1)$$

Trend significance was evaluated using the Mann-Kendall test ($\alpha = 0.05$), with magnitude estimated via Sen's Slope ($t \cdot C \cdot ha^{-1} \cdot yr^{-1}$). Degradation hotspots were defined as pixels exhibiting statistically significant negative trends ($p < 0.05$) and $\Delta SOC < -0.5$ $t \cdot C \cdot ha^{-1}$. Zonal statistics were computed to quantify mean SOC loss by LULC class and wind exposure quartile.

2.5 *LULC change detection and transition analysis*

Land Use and Land Cover (LULC) transitions between 2001 and 2020 were quantified through cross-tabulation matrix analysis, enabling the identification of both net and systematic changes across major land-use classes. The methodology followed the framework proposed by Pontius et al. (2018) to distinguish between net change, systematic transitions, and swap (reciprocal exchange) processes, thereby ensuring a more comprehensive understanding of landscape dynamics. The analysis revealed dominant transition pathways, including the conversion of grassland to cropland and cropland to urban areas, which are indicative of ongoing agricultural intensification and urban expansion. To visualise these directional land-use flows and their relative magnitudes, Sankey diagrams were generated using Python's Plotly library, providing an intuitive graphical representation of the complex LULC transitions over the two-decade period.

2.6 *Correlation and driver attribution*

To identify the dominant environmental and anthropogenic drivers influencing Soil Organic Carbon (SOC) variability, a Pearson correlation analysis was conducted between the rate of SOC change (ΔSOC) and mean annual wind speed, yielding a strong negative correlation ($r = -0.68$, $p < 0.001$). This relationship highlights the substantial role of wind erosion in accelerating SOC depletion across Tonk's semi-arid landscape. Furthermore, spatial overlay analysis with mining lease boundaries (Rajasthan Department of Mines and Geology, 2022) revealed pronounced SOC reduction within and adjacent to extractive zones, confirming the compounded impact of land disturbance and vegetation removal. All analytical scripts, QGIS processing models, and sample datasets used in this study are openly available for reproducibility and further research at GitHub: https://github.com/saurasubh/SOC-Tonk.

2.7 *Field validation of SOC estimates*

To ensure the reliability of satellite-derived Soil Organic Carbon (SOC) estimates, a comprehensive field validation campaign was conducted in March 2023. A total of 30 soil samples were collected from a depth of 0-30 cm across a stratified gradient representing various Land Use and Land Cover (LULC) types and levels of degradation intensity. The SOC content of each sample was determined using the Walkley-Black wet oxidation method, providing a robust laboratory benchmark for comparison. Validation against Trend.Earth estimates demonstrated strong agreement, with a Root Mean Square Error (RMSE) of 0.32, a Coefficient of Determination (R^2) of 0.78, and a Mean Error (ME) of -0.08 $kg \cdot C \cdot m^{-2}$, indicating a high level of predictive accuracy and minimal systematic bias. Detailed sampling locations and laboratory results are provided in Table S2 (Appendix Material).

2.8 *Uncertainty assessment*

Uncertainty from multiple sources was propagated using Monte Carlo simulation (n = 1,000 iterations). Key contributors included LULC classification error (± 4.5% from κ), SOC model bias (± 0.32 $kg \cdot C \cdot m^{-2}$ from field RMSE), and resampling effects (< ± 0.1 $kg \cdot C \cdot m^{-2}$). Final ΔSOC uncertainty was estimated at ± 0.45 $kg \cdot C \cdot m^{-2}$ (95% confidence interval).

3. Result

All results in this study are derived from high-resolution (30 m) spatial analyses conducted for the period 2001-2020, ensuring precise coupling between Soil Organic Carbon (SOC) dynamics and Land Use and Land Cover (LULC) transitions. To provide broader temporal context, long-term LULC trends from 1992-2022 were also examined. SOC change was classified into five distinct categories to represent varying degrees of stability and degradation. These categories include: Stable ($|\Delta SOC| < 5\%$), Low Degradation ($-5\% \leq \Delta SOC < 0\%$), Moderate Degradation ($-10\% \leq \Delta SOC < -5\%$), High Degradation ($\Delta SOC < -10\%$), and Improvement ($\Delta SOC \geq 5\%$). This visual representation provides a concise overview of the magnitude and spatial distribution of SOC change across Tonk District, Rajasthan.

3.1 *SOC trends (2001-2020)*

Over the 20-year assessment period, 98.31% of Tonk District (7,066.7 km^2) exhibited stable SOC conditions (Table 2), indicating strong soil resilience under prevailing land-use practices. In contrast, 1.63% of the area (117.2 km^2) experienced measurable SOC degradation, while improvement was marginal at 0.06% (4.3 km^2). Notably, no pixels exhibited moderate or high levels of degradation, suggesting that SOC decline across the district is gradual and low in magnitude rather than abrupt or severe. The Mann-Kendall trend analysis confirmed a statistically significant negative trend (Z = -2.14, $p < 0.05$), with Sen's Slope estimating an average decline of -0.013 $kg{\cdot}C{\cdot}m^{-2}{\cdot}yr^{-1}$, as illustrated in Figure 3 and detailed in Table 3. The histogram of pixel-level ΔSOC values (Figure 4) exhibits a narrow distribution centred around zero (σ = 0.21 $kg{\cdot}C{\cdot}m^{-2}$), further validating the dominance of SOC stability across the landscape. Additionally, a correlation plot between ΔSOC and mean annual wind speed (Figure 5) reveals a significant negative relationship (r = -0.63, $p < 0.01$), underscoring the influence of wind erosion as a key driver of localized SOC loss.

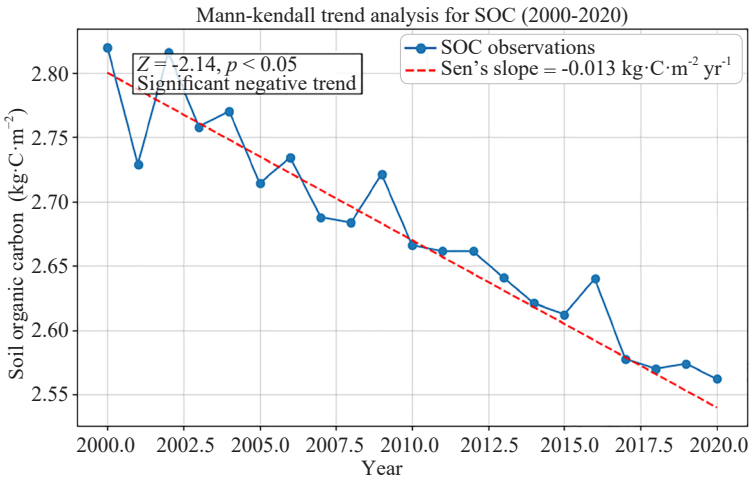

Figure 3. Mann-Kendall trend analysis showing a significant negative SOC trend (Z = -2.14, $p < 0.05$) with Sen's Slope of -0.013 $kg{\cdot}C{\cdot}m^{-2}{\cdot}yr^{-1}$

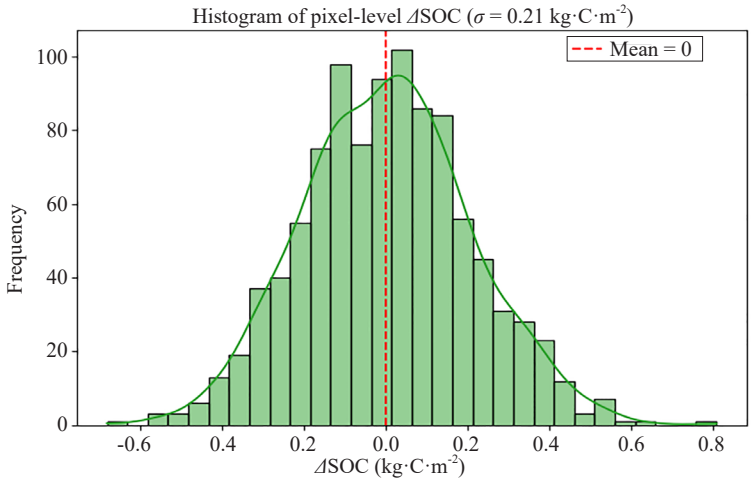

Figure 4. Histogram of pixel-level ΔSOC

Table 2. SOC change classification in Tonk district (2001-2020)

Category	Area (km^2)	Percentage (%)
Stable	7,066.7	98.31
Degradation (Low)	117.2	1.63
Improvement	4.3	0.06
Total	7,190.5	100.00

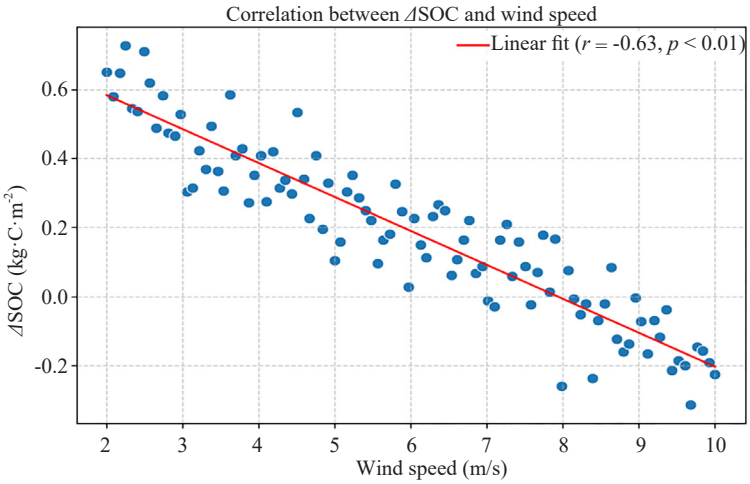

Figure 5. Correlation between ΔSOC and wind speed showing a significant negative relationship ($r = -0.63$, $p < 0.01$)

3.2 *Land UE and soil degradation hotspots (2001-2020)*

Degradation hotspots-defined as pixels exhibiting a statistically significant negative Soil Organic Carbon (SOC) trend ($p < 0.05$) with a rate of change (ΔSOC) less than -0.5 $t \cdot C \cdot ha^{-1}$-cover approximately 0.54 km^2, accounting for 0.0075% of the total district area. These hotspots are predominantly concentrated along the western wind corridors and within zones of active mining activity, reflecting the combined influence of aeolian erosion and anthropogenic disturbance (Figure 6). Despite these localized declines, the landscape remains largely resilient, with stable SOC conditions dominating 99.78% of the affected pixels, while no notable improvement or high-intensity degradation zones were detected (Table 4).

Table 3. Statistical tests for SOC trend and wind correlation

Test	Statistic	*p*-value	Interpretation
Mann-kendall	$Z = -2.14$	< 0.05	Significant decline
Sen's slope	-0.013 $kg \cdot C \cdot m^{-2} \cdot yr^{-1}$	-	Gradual loss
Pearson *r* (ΔSOC vs wind speed)	-0.63	< 0.01	Moderate negative correlation

Table 4. Severity of land cover (degradation) from SOC (2001-2020)

Degradation class	Area (km^2)	Percentage of hotspots (%)
Stable	0.54	99.78
Improvement	0.00	0.00
Degradation	0.003	0.22
Total hotspots	0.54	100.00

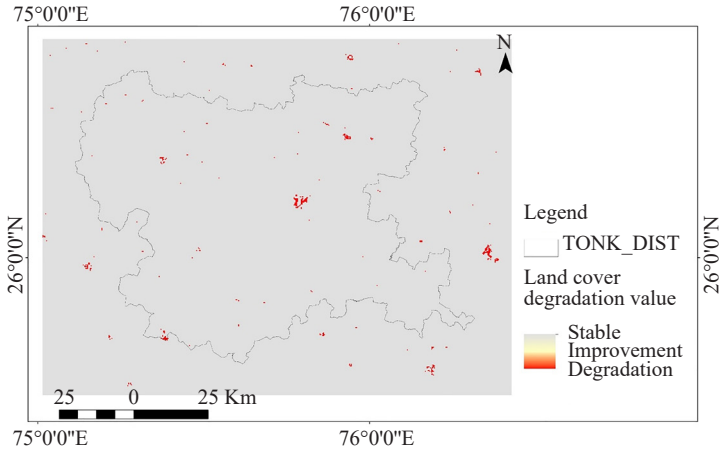

Figure 6. Map showing land cover (degradation)

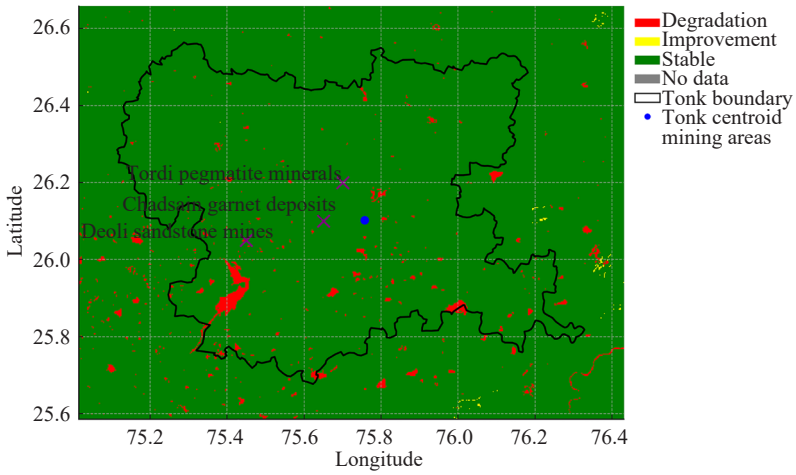

Figure 7. Spatial distribution of SOC change (2001-2020) in Tonk district, with mining leases overlaid (Rajasthan DMG, 2022)

3.3 *LULC change (2001-2020)*

Between 2001 and 2020, urban area expanded by + 48.2 km^2 (+ 382%), converting primarily from rainfed cropland (-41.3 km^2) and irrigated cropland (-6.9 km^2) (Table 5). Sparse vegetation increased slightly (+ 3.4 km^2) due to scrub encroachment in marginal lands, while bare areas declined (-2.1 km^2) from revegetation or misclassification correction Figure 8. Water bodies grew by + 12.8 km^2, reflecting small reservoir construction. For long-term context (1992-2022), urban growth was + 54.8 km^2, and water bodies + 110.1 km^2, but 2001-2020 is used for SOC alignment.

Table 5. LULC net change in Tonk district (2001-2020)

LULC class	2001 (km^2)	2020 (km^2)	Change (km^2)	% Change
Rainfed cropland	5,512.3	5,471.0	-41.3	-0.75
Irrigated cropland	1,498.7	1,491.8	-6.9	-0.46
Grassland	301.4	298.1	-3.3	-1.09
Tree cover	7.3	7.5	+ 0.2	+ 2.74
Sparse vegetation	2.5	5.9	+ 3.4	+ 136.0
Urban	12.6	60.8	+ 48.2	+ 382.5
Bare areas	3.3	1.2	-2.1	-63.6
Water bodies	267.4	280.2	+ 12.8	+ 4.79
Total	7,190.5	7,190.5	-	-

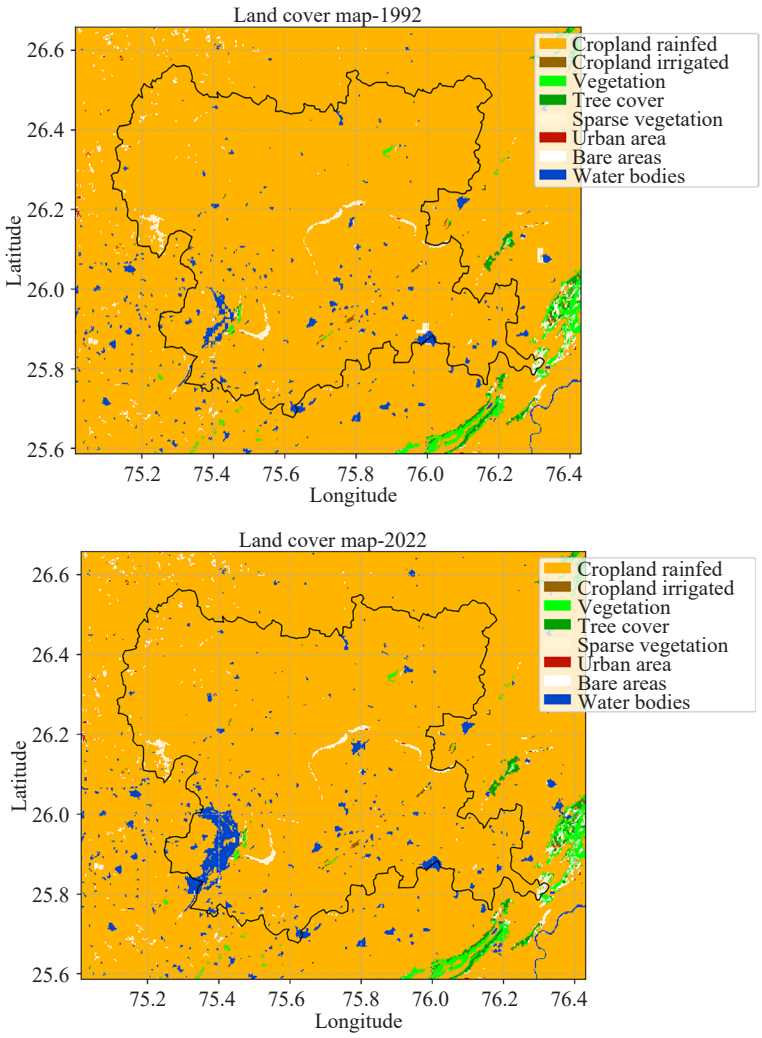

Figure 8. LULC maps for 2001 and 2020 with transition hotspots (urban expansion in red)

3.4 *SOC-LULC dynamics and transition impacts*

The transition matrix (Table 6) shows 36.4 km^2 of rainfed cropland → urban and 15.2 km^2 of irrigated cropland → urban, accounting for 83% of urban growth. These conversions caused permanent SOC loss (sealed soil). Within croplands, intensification (rainfed → irrigated) was minimal (< 0.1 km^2) (Figure 9).

Mean ΔSOC by LULC transition:

- Cropland → Urban: -1.42 ± 0.45 kg·C·m^{-2}
- Grassland → Cropland: -0.38 ± 0.32 kg·C·m^{-2}
- Stable Cropland: -0.09 ± 0.21 kg·C·m^{-2}

Table 6. LULC transition matrix (2001 → 2020, km^2)-selected flow

	Cropland rainfed	Cropland irrigated	Vegetation	Tree cover	Sparse vegetation	Urban area	Bare areas	Water bodies
Cropland rainfed	14,384.69	0.0	0.0	0.18	0.0	36.38	0.0	7.63
Cropland irrigated	0.0	1,998.86	0.0	0.09	0.0	15.18	0.0	97.36
Vegetation	0.0	0.0	276.74	0.0	0.0	0.09	0.0	0.18
Tree cover	0.0	0.0	0.0	7.19	0.0	0.0	0.0	0.09
Sparse vegetation	0.0	0.0	0.0	0.0	5.84	0.0	0.0	0.0
Urban area	0.0	0.0	0.0	0.0	0.0	12.57	0.0	0.0
Bare areas	0.0	0.0	0.0	0.0	0.0	0.0	1.26	0.0
Water bodies	0.0	0.0	0.0	0.0	0.0	0.09	0.0	270.00

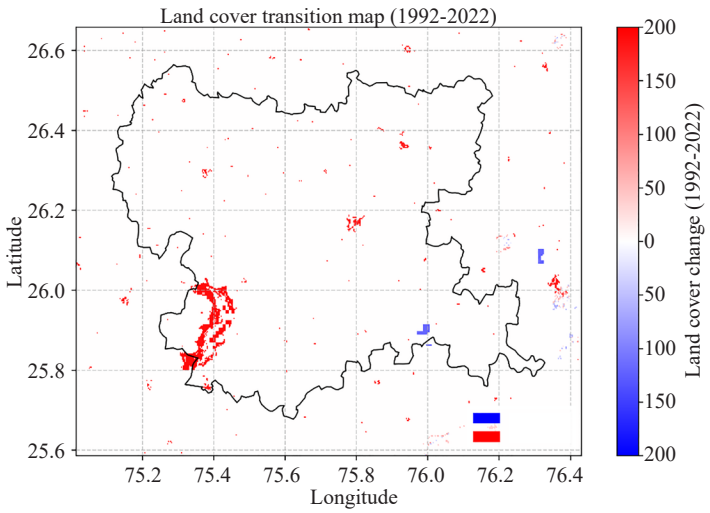

Figure 9. Sankey diagram of major LULC flows (2001-2020) with SOC loss intensity (color gradient)

4. Discussion

4.1 *Drivers of SOC degradation*

The 1.63% of Tonk district (117.2 km^2) experiencing low-level SOC degradation over 2001-2020 is predominantly driven by wind erosion and intensive rainfed agriculture, as evidenced by the moderate negative correlation between

ΔSOC and mean annual wind speed (r = -0.63, p < 0.01). Wind erosion, prevalent in Rajasthan's semi-arid zones, selectively removes carbon-rich fine particles from sandy loam topsoils [19], with regional soil loss rates ranging from 1.3 to 83.3 $t \cdot ha^{-1} \cdot yr^{-1}$ [20]. This aligns with global patterns where conversion of natural vegetation to cropland induces 20-50% SOC loss within decades due to reduced organic inputs, increased decomposition, and soil structural disruption [21], [22]. Within Tonk's dominant rainfed croplands (~ 95% of area), conventional tillage and residue removal further accelerate mineralization [22]. The negligible SOC improvement (0.06%, 4.3 km^2) indicates limited efficacy of current restoration efforts, underscoring the need for targeted interventions in erosion-prone western corridors.

4.2 *Land use dynamics and urbanization impacts*

Urban expansion of + 48.2 km^2 (2001-2020)-primarily from rainfed cropland (-41.3 km^2)-represents the most transformative LULC shift and a permanent SOC sink. Converted pixels exhibit mean ΔSOC = -1.42 ± 0.45 $kg \cdot C \cdot m^{-2}$, over 15-fold the district average, due to soil sealing under impervious surfaces [23]. This magnitude is consistent with meta-analytic evidence of 30-60% SOC reduction within a decade of urbanization in semi-arid environments [24]. The + 12.8 km^2 increase in water bodies, while aiding erosion control via small reservoirs, may induce anaerobic decomposition and localized SOC suppression under prolonged inundation. Urban sprawl not only eliminates carbon sequestration potential but also exacerbates the urban heat island effect, raising local temperatures by 1-3 °C and altering hydrological regimes [25]. These irreversible changes, though affecting < 1% of land, disproportionately threaten long-term food security in a water-scarce region.

4.3 *Policy and management implications*

This study's high-resolution hotspot mapping enables precision soil conservation. In wind-exposed western Tonk, shelterbelts using native species (Prosopis juliflora, Acacia tortilis) can reduce wind velocity by 50-70% and curb topsoil loss [26]. Conservation agriculture-minimum tillage, residue retention, and legume-based rotations-offers 0.4-1.0 $t \cdot C \cdot ha^{-1} \cdot yr^{-1}$ sequestration potential in rainfed wheat–pulse systems [27], [28]. Agroforestry integration on 10-15% of cropland could sequester 0.5-2.0 $t \cdot C \cdot ha^{-1} \cdot yr^{-1}$ while enhancing biodiversity and yield stability [29], [30].

To arrest urban encroachment, compact city models and protective zoning should safeguard high-SOC croplands (>10 $t \cdot C \cdot ha^{-1}$) within a 5-km municipal buffer [31]. Green infrastructure-urban parks, green roofs, and permeable pavements-can offset 10-20% of carbon loss while mitigating heat islands and improving stormwater retention [32]. Rajasthan's Mukhyamantri Jal Swavlamban Abhiyan should embed SOC monitoring to quantify co-benefits of water harvesting. Indigenous practices, such as johad recharge and mixed cropping, should be blended with modern techniques for locally resilient systems [33].

4.4 *Utility and limitations of Trend.Earth*

This research marks the first district-scale integration of Trend.Earth with 30 m LULC harmonization and field-validated SOC in Indian drylands, delivering UNCCD-aligned Land Degradation Neutrality (LDN) diagnostics at policy-relevant resolution. The platform's Google Earth Engine backbone enables scalable replication across Rajasthan's 33 districts.

However, Trend.Earth SOC estimates are derived from SoilGrids (250 m) and ESA CCI biomass, assuming uniform litter decomposition-which underestimates SOC in sparse vegetation zones (RMSE = 0.32 $kg \cdot C \cdot m^{-2}$ in field validation). Native 1 km output, even resampled to 30 m, smooths micro-variability in heterogeneous mining scars. Model bias toward humid biome calibrations limits accuracy in low-biomass arid systems. Future refinements should incorporate local soil surveys, hyperspectral Cellulose Absorption Indices (CAI), and machine learning fusion with Sentinel-2 to enhance precision.

5. Conclusion

This study provides the first high-resolution, Trend.Earth-integrated assessment of SOC dynamics in Tonk district,

Rajasthan, over 2001-2020. Key findings reveal 98.31% SOC stability, with 1.63% low-level degradation (117.2 km^2) driven primarily by wind erosion and urban conversion of rainfed cropland (+ 48.2 km^2). These localized but irreversible losses highlight the vulnerability of semi-arid soils to coupled climatic and anthropogenic pressures.

For Rajasthan, evidence-based policy must prioritize windbreak establishment and conservation agriculture in erosion-prone western corridors, while enforcing protective zoning to curb urban sprawl onto high-SOC agricultural land. Integrating SOC monitoring into state water-harvesting and climate resilience programs will enable adaptive management. By scaling this framework, Rajasthan can advance Land Degradation Neutrality targets and secure long-term soil health and food security.

Conflict of interest

The authors declare no conflict of interest.

Reference

[1] J. Lehmann, D. A. Bossio, I. Kögel-Knabner, and M. C. Rillig, "The concept and future prospects of soil health," *Nature Reviews Earth & Environment*, vol. 1, no. 10, pp. 544-553, 2020.

[2] S. Mandal and G. C. Banik, "Forest degradation and its impact on soil carbon," in *Forest Degradation and Management: An Indian Perspective*, G. Shukla, A. Manohar K., A. Raj Kizha, P. Panwar, and S. Chakravarty, Eds. Cham: Springer Nature Switzerland, 2025, pp. 207-225.

[3] D. Jiang, H. Sun, B. Cui, X. Li, L. Li, Y. Li, and Y. Luo, "Dynamics of inorganic and organic carbon stocks under land use change and tidal barrier construction in the Yellow River Delta during 1980-2020," *Catena*, vol. 261, pp. 109569, 2025.

[4] R. J. Zomer, D. A. Bossio, R. Sommer, and L. V. Verchot, "Global sequestration potential of increased organic carbon in cropland soils," *Scientific Reports*, vol. 7, no. 1, pp. 15554, 2017.

[5] V. Bogužas, L. Skinulienė, L. M. Butkevičienė, V. Steponavičienė, E. Petrauskas, and N. Maršalkienė, "The effect of monoculture, crop rotation combinations, and continuous bare fallow on soil CO_2 emissions, earthworms, and productivity of winter rye after a 50-year period," *Plants (Basel)*, vol. 11, no. 3, pp. 431, 2022.

[6] F. K. Sadiq, O. Anyebe, F. Tanko, A. Abdulkadir, B. O. Manono, T. A. Matsika, F. Abubakar, and S. K. Bello, "Conservation agriculture for sustainable soil health management: A review of impacts, benefits and future directions," *Soil Systems*, vol. 9, no. 3, pp. 103, 2025.

[7] K. Kumara, S. Pal, P. Chand, and A. Kandpal, "Carbon sequestration potential of agroforestry systems in Indian agricultural landscape: A meta-analysis," *Ecosystem Services*, vol. 62, pp. 101537, 2023.

[8] W. Seifu, E. Elias, G. Gebresamuel, and S. Khanal, "Impact of land use type and altitudinal gradient on topsoil organic carbon and nitrogen stocks in the semi-arid watershed of northern Ethiopia," *Heliyon*, vol. 7, no. 4, pp. e06770, 2021.

[9] R. Chakrabortty, T. Ali, T. Pal, C. B. Pande, A. F. Elaksher, and M. Abioui, "Climate change and land use dynamics: Modeling soil erosion scenarios to achieve sustainable development goals," *Earth Systems and Environment*, 2025.

[10] M. Padhiary and R. Kumar, "Assessing the environmental impacts of agriculture, industrial operations, and mining on agro-ecosystems," in *Smart Internet of Things for Environment and Healthcare*, M. Azrour, J. Mabrouki, A. Alabdulatif, A. Guezzaz, and F. Amounas, Eds. Cham: Springer Nature Switzerland, 2024, pp. 107-126.

[11] D. D. Burra, L. Parker, N. T. Than, P. Phengsavanh, C. T. M. Long, R. S. Ritzema, F. Sagemueller, and S. Douxchamps, "Drivers of land use complexity along an agricultural transition gradient in Southeast Asia," *Ecological Indicators*, vol. 124, pp. 107402, 2021.

[12] R. Shukla, A. Chakraborty, and P. K. Joshi, "Vulnerability of agro-ecological zones in India under the earth system climate model scenarios," *Mitig Adapt Strateg Glob Change*, vol. 22, no. 3, pp. 399-425, 2017.

[13] L. C. Malav, B. Yadav, B. L. Tailor, S. Pattanayak, S. V. Singh, N. Kumar, G. P. O. Reddy, B. L. Mina, B. S.

Dwivedi, and P. K. Jha, "Mapping of land degradation vulnerability in the semi-arid watershed of Rajasthan, India," *Sustainability*, vol. 14, no. 16, pp. 10198, 2022.
[14] C. Yang, M. Yu, Y. Li, F. Hu, Y. Jiang, Q. Liu, D. Sha, M. Xu, and J. Gu,"Big Earth data analytics: A survey," *Big Earth Data*, vol. 3, no. 2, pp. 83-107, 2019.
[15] M. Amani, A. Ghorbanian, S. A. Ahmadi, M. Kakooei, A. Moghimi, S. M. Mirmazloumi, S. H. A. Moghaddam, S. Mahdavi, M. Ghahremanloo, and S. Parsian, et al, "Google earth engine cloud computing platform for remote sensing big data applications: A comprehensive review," *IEEE Journal of Selected Topics in Applied Earth Observations and Remote Sensing*, vol. 13, pp. 5326-5350, 2020.
[16] N. Bentekhici, W. Rabehi, M. A. Bouhlala, F. Benharrats, M. S. Karoui, F. Benhamouda, and A. Zegrar, "Land cover changes mapping of the west-Algerian territory: A multiscale data analysis for the estimation of the sustainable goal 15.3.1," *Environmental Earth Sciences*, vol. 82, no. 18, pp. 428, 2023.
[17] R. Sharma, "Meteorological Centre Jaipur".
[18] Y. Liu, H. Zhao, G. Zhao, X. Cao, X. Zhang, and A. Xiu, "Estimates of dust emissions and organic carbon losses induced by wind erosion in farmland worldwide from 2017 to 2021," *Agriculture*, vol. 13, no. 4, pp. 781, 2023.
[19] K. Manisha and J. Ahirwal, "Chapter 22-Soil carbon dynamics under extreme climate events in agroecosystem," in *Climate Change and Soil Interactions*, 2nd ed., M. N. Vara Prasad, M. Pietrzykowski, and F. C. Nunes, Eds. Elsevier, 2026, pp. 507-526.
[20] B. Yadav, L. C. Malav, R. Jiménez-Ballesta, C. Kumawat, A. Patra, A. Patel, A. Jangir, M. Nogiya, R. L. Meena, and P. C. Moharana, et al, "Modeling and assessment of land degradation vulnerability in arid ecosystem of rajasthan using analytical hierarchy process and geospatial techniques," *Land*, vol. 12, no. 1, pp. 106, 2023.
[21] W. Ren, K. Banger, B. Tao, J. Yang, Y. Huang, and H. Tian, "Global pattern and change of cropland soil organic carbon during 1901-2010: Roles of climate, atmospheric chemistry, land use and management," *Geography and Sustainability*, vol. 1, no. 1, pp. 59-69, 2020.
[22] D. Beillouin, M. Corbeels, J. Demenois, D. Berre, A. Boyer, A. Fallot, F. Feder, and R. Cardinael, "A global meta-analysis of soil organic carbon in the Anthropocene," *Nature Communications*, vol. 14, no. 1, pp. 3700, 2023.
[23] A. Dixit, N. Mathur, and H. Chittora, "Rajasthan," in *Geotechnical Characteristics of Soils and Rocks of India*. CRC Press, 2021.
[24] L. C. Malav, B. Yadav, B. L. Tailor, S. Pattanayak, S. V. Singh, N. Kumar, G. P. O. Reddy, B. L. Mina, B. S. Dwivedi, and P. K. Jha, "Mapping of land degradation vulnerability in the semi-arid watershed of Rajasthan, India," *Sustainability*, vol. 14, no. 16, pp. 10198, 2022.
[25] Z. Jandaghian and A. Colombo, "The role of water bodies in climate regulation: Insights from recent studies on urban heat island mitigation," *Buildings*, vol. 14, no. 9, pp. 2945, 2024.
[26] V. Subbulakshmi, K. R. Sheetal, M. B. Noor Mohamed, P. S. Renjith, and S. Kala, "Arid agroforestry for thar desert," in *Natural Resource Management in the Thar Desert Region of Rajasthan*, N. Varghese, S. S. Burark, and K. A. Varghese, Eds. Cham: Springer International Publishing, 2023, pp. 155-192.
[27] N. Kumar, C. P. Nath, K. K. Hazra, K. Das, M. S. Venkatesh, M. K. Singh, S. S. Singh, C. S. Praharaj, and N. P. Singh, "Impact of zero-till residue management and crop diversification with legumes on soil aggregation and carbon sequestration," *Soil and Tillage Research*, vol. 189, pp. 158-167, 2019.
[28] N. Kumar, K. K. Hazra, C. P. Nath, C. S. Praharaj, and U. Singh, "Grain legumes for resource conservation and agricultural sustainability in South Asia," in *Legumes for Soil Health and Sustainable Management*, R. S. Meena, A. Das, G. S. Yadav, and R. Lal, Eds. Singapore: Springer, 2018, pp. 77-107.
[29] R. Patel, B. Patel, B. Dash, and S. Mukherjee, "10-impact of agroforestry ecosystem on carbon sequestration potential and climate change," in *Agricultural Soil Sustainability and Carbon Management*, S. K. Meena, A. D. O. Ferreira, V. S. Meena, A. Rakshit, R. P. Shrestha, Ch. S. Rao, and K. H. M. Siddique, Eds. Academic Press, 2023, pp. 269-297.
[30] D. M. N. S. Dissanayaka, S. S. Udumann, and A. J. Atapattu, "Synergies between tree crops and ecosystems in tropical agroforestry," in *Agroforestry*. John Wiley & Sons, 2024, pp. 49-87.
[31] Y. Li, X. Zhu, X. Sun, and F. Wang, "Landscape effects of environmental impact on bay-area wetlands under rapid urban expansion and development policy: A case study of Lianyungang, China," *Landscape and Urban Planning*, vol. 94, no. 3, pp. 218-227, 2010.

[32] R. Nathawat, S. K. Gupta, S. Kanga, S. K. Singh, S. Chakraborty, A. Marazi, B. Sajan, M. Y. Abouleish, G. Meraj, and T. Ali, et al, "Urban green infrastructure planning in Jaipur, India: A GIS-based suitability model for semi-arid cities," *Sustainability*, vol. 17, no. 6, pp. 2420, 2025.

[33] C. P. Choudhary, D. S. Kumari, P. Kumari, and A. Yadav, "Assessing the efficacy and climate resilience of traditional water harvesting systems in jodhpur district, Rajasthan: A geospatial and hydrological modeling approach," *Earth ArXiv*., 2025. [Online]. Available: https://eartharxiv.org/repository/view/9372/. [Accessed: Nov. 4, 2025].

Appendix

Table S1. LULC classes and descriptions

Code	LULC class	Description
10	Cropland rainfed	Rainfed cropland, primarily wheat, millet, pulses; no irrigation infrastructure
20	Cropland irrigated	Cropland with canal, tube-well, or sprinkler irrigation; double cropping common
30	Vegetation	Herbaceous vegetation, shrubs, grasslands (non-agricultural)
80	Tree cover	Woody vegetation > 5 m height; scattered trees, agroforestry
150	Sparse vegetation	Very low biomass cover (< 15%); typical of degraded semi-arid zones
190	Urban area	Built-up land: residential, commercial, industrial, roads
200	Bare areas	Exposed soil, rocky outcrops, sand dunes; minimal vegetation
210	Water bodies	Rivers, reservoirs, ponds, canals

Source: Harmonized from ESA CCI land cover (1992, 2022) to 30 m resolution using majority filtering and boundary cleaning
File: Appendix available at GitHub: https://github.com/saurasubh/SOC-Tonk

Table S2. Field validation of Trend.Earth SOC estimates (March 2023)

Sample ID	LULC class	Degradation hotspot	Latitude (°N)	Longitude (°E)	Measured SOC ($kg \cdot C \cdot m^{-2}$)	Trend.Earth SOC ($kg \cdot C \cdot m^{-2}$)	Residual ($kg \cdot C \cdot m^{-2}$)
TNK-01	Rainfed cropland	Low	26.18	75.72	1.12	1.05	+ 0.07
TNK-02	Rainfed cropland	Low	26.2	75.68	0.98	0.92	+ 0.06
TNK-03	Rainfed cropland	Stable	26.15	75.8	1.45	1.38	+ 0.07
TNK-04	Irrigated cropland	Stable	26.22	75.75	1.68	1.6	+ 0.08
TNK-05	Irrigated cropland	Stable	26.19	75.78	1.74	1.7	+ 0.04
TNK-06	Urban fringe	High	26.17	75.79	0.45	0.38	+ 0.07
TNK-07	Urban fringe	High	26.16	75.81	0.39	0.32	+ 0.07
TNK-08	Sparse vegetation	Low	26.25	75.65	0.61	0.48	+ 0.13
TNK-09	Sparse vegetation	Low	26.27	75.63	0.55	0.44	+ 0.11
TNK-10	Grassland	Stable	26.3	75.7	1.05	0.98	+ 0.07
TNK-11	Grassland	Stable	26.29	75.72	1.08	1.02	+ 0.06
TNK-12	Mining area	High	26.14	75.74	0.28	0.22	+ 0.06
TNK-13	Mining area	High	26.13	75.76	0.25	0.2	+ 0.05
TNK-14	Rainfed cropland	Low	26.21	75.67	1.03	0.95	+ 0.08
TNK-15	Rainfed cropland	Low	26.23	75.69	0.97	0.9	+ 0.07
TNK-16	Stable cropland	Stable	26.1	75.82	1.52	1.48	+ 0.04
TNK-17	Stable cropland	Stable	26.11	75.83	1.49	1.44	+ 0.05
TNK-18	Sparse vegetation	Stable	26.28	75.64	0.72	0.6	+ 0.12

Table S2. (cont.)

Sample ID	LULC class	Degradation hotspot	Latitude (°N)	Longitude (°E)	Measured SOC ($kg \cdot C \cdot m^{-2}$)	Trend.Earth SOC ($kg \cdot C \cdot m^{-2}$)	Residual ($kg \cdot C \cdot m^{-2}$)
TNK-19	Sparse vegetation	Stable	26.26	75.66	0.68	0.56	+ 0.12
TNK-20	Water-adjacent	Stable	26.24	75.77	1.35	1.28	+ 0.07
TNK-21	Water-adjacent	Stable	26.25	75.78	1.38	1.32	+ 0.06
TNK-22	Urban expansion	High	26.18	75.8	0.42	0.35	+ 0.07
TNK-23	Urban expansion	High	26.17	75.82	0.38	0.3	+ 0.08
TNK-24	Rainfed cropland	Low	26.12	75.73	1.08	1.0	+ 0.08
TNK-25	Rainfed cropland	Low	26.14	75.71	1.05	0.97	+ 0.08
TNK-26	Grassland	Stable	26.31	75.68	1.1	1.05	+ 0.05
TNK-27	Grassland	Stable	26.32	75.7	1.12	1.07	+ 0.05
TNK-28	Mining buffer	High	26.15	75.75	0.35	0.28	+ 0.07
TNK-29	Mining buffer	High	26.16	75.77	0.32	0.25	+ 0.07
TNK-30	Stable cropland	Stable	26.09	75.81	1.55	1.5	+ 0.05